Two-Parameter Analysis of Be^{10}, B^{11}, B^{12}, and B^{13} Spectra*

R. R. CARLSON AND E. NORBECK

Department of Physics, State University of Iowa, Iowa City, Iowa
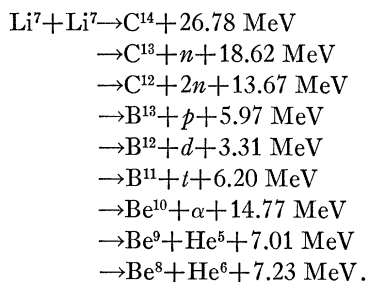
(Received 29 March 1963)

Bound states of Be^{10}, B^{11}, B^{12}, and B^{13} were formed by bombardment of Li^7 with 3-MeV Li^7 ions and were studied by two-parameter analysis. Gamma radiation from these states and particles associated with their production were measured in coincidence. A 256×256-channel two-parameter analyzer made up of a general purpose computer and two 256-channel pulse-height analyzers was used. The gamma-ray emission from individual bound states of the above nuclei was obtained uncontaminated by cascade feeding of levels. Gamma-ray branching ratios of levels in Be^{10} and B^{11} confirm previous measurements. Gamma-ray branching ratios of the bound levels of B^{12} and B^{13} were measured for the first time. The pattern of gamma-ray branching ratios of B^{13} bears a certain resemblance to that for B^{11}. The first excited state of B^{13} previously believed to be at 3.70 MeV was found to be a doublet at 3.50 ± 0.05 MeV and 3.70 ± 0.05 MeV.

INTRODUCTION

THE level structures of the boron isotopes have been the objects of a large number of studies.[1] The energies of the bound excited states are fairly well known. The spins and parities are best known for B^{11}. Gamma-ray branching ratios are also best known for B^{11}. Little is known about these quantities for the boron isotopes B^{12} and B^{13}. Gamma-ray branching ratios serve as a sensitive test of any nuclear model. They are sensitive to features of the model which may not show up in the calculation of energy level positions. The boron isotopes, being in the $1p$ shell, have a sufficiently low number of nucleons that gamma-ray branching ratios might be calculable. This work presents measured branching ratios for comparison. In order to collect the data, a new technique has been used in this work. It involves the use of a general purpose computer as a two-parameter analyzer for both collection and analysis of data.

The boron isotopes were produced by the bombardment of Li^7 targets by Li^7 beams. With 3-MeV Li^7 ions, the following reactions are possible:

$$
\begin{aligned}
Li^7 + Li^7 &\to C^{14} + 26.78 \text{ MeV} \\
&\to C^{13} + n + 18.62 \text{ MeV} \\
&\to C^{12} + 2n + 13.67 \text{ MeV} \\
&\to B^{13} + p + 5.97 \text{ MeV} \\
&\to B^{12} + d + 3.31 \text{ MeV} \\
&\to B^{11} + t + 6.20 \text{ MeV} \\
&\to Be^{10} + \alpha + 14.77 \text{ MeV} \\
&\to Be^9 + He^5 + 7.01 \text{ MeV} \\
&\to Be^8 + He^6 + 7.23 \text{ MeV}.
\end{aligned}
$$

In addition to these possibilities, there are also those cases where one or more of the residual nuclei may be replaced by their constituents; e.g., He^5 by α and n, or t by d and n.

It is the large mass excess of the lithium ions which gives rise to the richness of the result. The residual nuclei can be formed in all of their bound excited states and in a number of unbound excited states as well. This gives one a new and relatively unused means of forming nuclear states for study. The nature of the reaction mechanism involved in the various reactions above is a very interesting one but is not considered here. The lithium bombardment is simply used to produce the residual nuclei.

The richness of the result is somewhat embarrassing. The gamma radiation has been studied before,[2] but because of the complexity of the spectrum, it is difficult to assign gamma rays to their sources. Also gamma-ray branching ratios cannot be determined without knowledge of the relative population of the residual nuclear states. To determine gamma-ray branching ratios, therefore, gamma rays were measured in time coincidence with associated charged particles. From the list of reactions above, it can be seen that the requirement of (γ-charged particle) coincidence narrows the number of observed reactions down to those producing the boron isotopes and Be^{10}.

In order to unravel the complex gamma-ray spectrum, the requirement of coincidence above is necessary but not sufficient. The particle energies were also measured and a two-parameter pulse-height distribution accumulated. The two pulse heights were sorted into 256 channels each and the number of counts accumulated, in each of $256\times256 = 65\,536$ positions in the two-parameter pulse-height distribution, were stored. This was accomplished with a general purpose computer which was also used to condense, manipulate, and display the accumulated information. The combination of time coincidence and energy measurement makes possible the study of the gamma-ray decay of each nuclear energy level which is formed with sufficient intensity.

APPARATUS

The Li^7 beam was provided by the State University of Iowa Van de Graaff accelerator. Magnetic analysis of the beam determined the energy to about a percent.

[1] F. Ajzenberg-Selove and T. Lauritsen, Nucl. Phys. **11**, 1 (1959); in *Landolt-Börnstein Tables*, edited by K. H. Hellwege (Springer-Verlag, Berlin, 1961), New Series, Group 1, Vol. 1.

[2] E. Berkowitz, S. Bashkin, R. R. Carlson, S. A. Coon, and E. Norbeck, Phys. Rev. **128**, 247 (1962).

Beam currents were typically a few tenths of a micro-ampere of singly charged ions. The beam impinged on an evaporated Li⁷F target. By comparison with gamma-ray yields measured as a function of bombarding energy with an infinitely thick Li⁷F target and a Li⁷ beam, the evaporated targets were found to be about 100-keV thick to a 3-MeV Li⁷ beam. These evaporated targets were deposited on 3.1 mg/cm² aluminum foil which is thin enough so that no large energy losses occur for the outgoing charged particles of interest. The target backing did, however, stop the beam particles which had an energy of 3.0 MeV.

Observations were made with a target chamber having cylindrical shape with its axis at right angles to the beam direction and intersecting it. The chamber diameter was 10 cm. The chamber is shown schematically in Fig. 1. The target was held at right angles to the beam on the chamber axis (this angle could be varied). A solid-state particle detector was located inside the cylinder in the vacuum. It could be rotated from 0° with respect to the beam to 140° with respect to the beam. It was kept at 0° throughout most of the experiment. The particle detector's sensitive area was 5-mm×5-mm square and this area was at right angles to a line joining the detector and the beam spot on the target. The beam spot to detector distance was 20 mm. The detector was housed inside of an electrically shielded housing and aluminum foils of various thicknesses could be placed over the detector face at will to make possible the identification of charged particles on the basis of different energy losses in the various foils. These foils also served to give complete electrical shielding and eliminate effects of light on the detectors. A 1.3 mg/cm² aluminum foil was kept over the detector in most of the work reported here. A natural α emitter could be placed in front of the detector at will to calibrate the particle detector system.

A 12.5-cm-diam by 15.0-cm-long NaI(Tl) crystal was used to detect the gamma radiation. The crystal axis intersected the chamber axis at the beam spot. The crystal could be moved in the same horizontal plane as
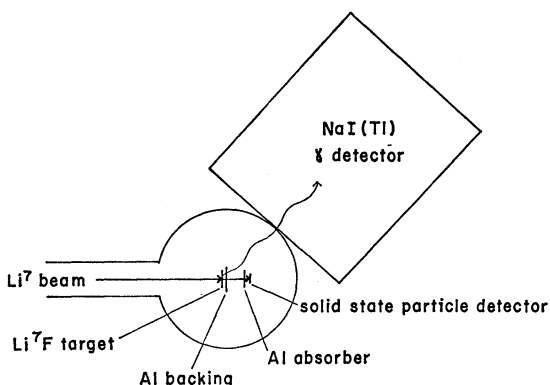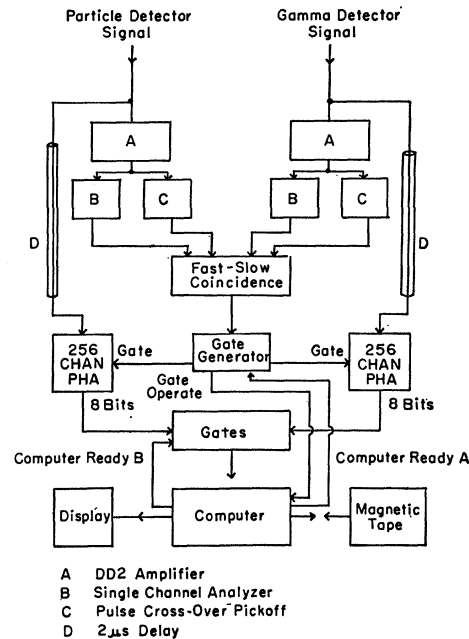

FIG. 2. Block diagram of electronic circuitry used to collect data using the two-parameter-analysis technique with a general purpose computer.

the charged particle from a position where its axis coincided with the beam direction to one where an angle of 135° was between them. It was usually kept at 45° here. The front face of the crystal could be brought to any distance from 5.1 to 30 cm from the beam spot on the target. It was usually kept at 5.5 cm here. Relatively little gamma-ray absorbing material came between the target spot and the crystal. Other than the target backing, there was only the 1.6-mm-thick brass wall of the chamber itself and the 0.75-mm-thick aluminum can in which the NaI(Tl) crystal was potted. With this amount of material, there is negligible difference in the amount of radiation absorbed over the range of gamma rays of interest here. However, since some distortion of the pulse-height distribution is possible and one object was to obtain relative gamma-ray intensities, gamma-ray pulse-height distributions were measured for gamma-ray sources through the same amount of material. These measured gamma-ray pulse-height distributions were used as standard shapes to decompose pulse-height distributions and obtain relative intensities. The sources were ThC″ for 2.62 MeV, B¹¹(p,γ)C¹² at 163 keV for 4.43 and 11.67 MeV, and F¹⁹($p,\alpha\gamma$)O¹⁶ for 6.13 MeV.

ELECTRONICS

Figure 2 shows the electronics used in schematic form. All electronic equipment, with the exception of the gate generator, the gate circuit, and the display circuit, was conventional and commercial. The gate generator, gate, and display circuits were constructed for their particular purpose here.

FIG. 1. Schematic diagram of target chamber, particle detector, and gamma-ray detector.
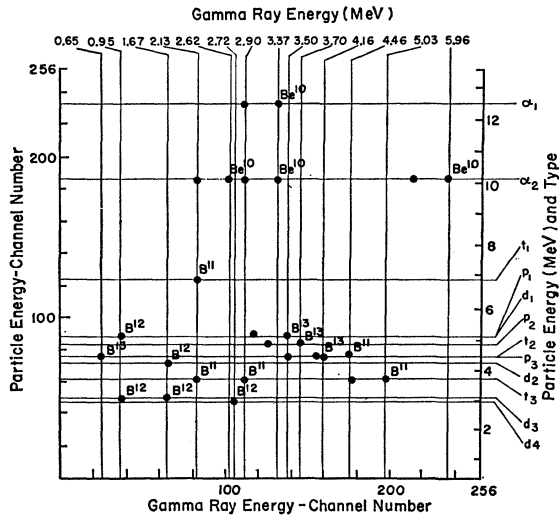
FIG. 3. Schematic diagram of two-parameter data. Each parameter is the output of a 256-channel analyzer when the two analyzers are in coincidence. The points represent peaks in the number of coincident counts at a pair of analyzer channels. The peaks are labeled by the residual nucleus giving off the gamma radiation detected. Coordinates for the peaks are labeled in channels and also gamma-ray energy and detected particle energy and type. Unlabeled peaks correspond to one-escape peaks.

The two time-coincident signals from the particle detector and the gamma-ray detector were each passed through DD2 amplifiers and the pulse cross-overs were picked off and used to determine fast coincidence in the fast-slow coincidence circuit to 50 nsec resolving time. Single channel analyzers on each detector signal were used to define the pulse-height region of interest. In the present experiment, these were set with very wide windows so as to include particles of energy from about 1.5 to about 15 MeV and gamma rays from about 0.5 to 7.5 MeV. The coincidence output signal caused the gate generator to operate if the computer had at any time previously put out a signal on the "computer ready A" line. The gate generator then gated both 256-channel pulse-height analyzers into operation and the two delayed signals from the two detectors were analyzed.

The computer was signaled by the "gate-operate" signal that an event was being analyzed. After a delay of 140 μsec to allow the two 256-channel analyzers to be certain of completing their jobs, the computer put signals on the "computer ready B" line and left other tasks which it may have been doing, such as displaying previously accumulated data. The signals operated gates which passed 8 bits at a time from each 256-channel analyzer successively into the computer.

The computer is a general purpose computer rented from the Control Data Corporation.[3] It is the CDC 160 model. It has 4096 words of 12 bits each and a cycle operation time of 6.4 μsec. This computer has been used

in a number of different ways in the course of this experiment alone, not to mention other experiments with which it is being used. The magnetic tape was handled in two CDC 164 tape units. These units have a reading and writing speed of 15 000 frames/sec.

In this experiment, the two pulse heights were temporarily stored until a sufficient number accumulated to dump the pairs of 8-bit pulse heights onto magnetic tape for permanent storage. The pairs of 8-bit numbers were also compressed by dropping 2 bits and using the 4096-word computer memory as a pulse-height analyzer memory. A pair of 6-bit numbers then defines the 12-bit address of the location where the count is stored. Reserving 4×64 or 256 words for program and temporary storage of 8-bit numbers, one ends with a direct-storage two-parameter analyzer with 60×64 or 3840 channels each capable of storing 4096 counts. In this mode of operation, about 500 μsec is required to analyze and store each event in the computer and on tape. The tape, of course, has no limit as to number of counts capable of being stored other than the time required, at a later time, to process the tape. As used, the tape stored the two pulse heights in full detail obtained from the two 256-channel analyzers giving 65 536-channel two-parameter pulse-height analysis capability.

The direct storage aspect of the data accumulation, while it does not appear in the final result, was of upmost usefulness in setting up the experiment and determining gain settings of the various amplifiers. The program called for display of these data in the form of a contour map. The computer memory was scanned, when no data storage was underway, and whenever a channel was found which had a number of counts equal to or greater than a given number, a bright spot was placed on an oscilloscope in the display. The spots appeared in a 60×64 matrix. Particle detector pulse height was displayed along the "60" direction and gamma-ray detector pulse height was displayed along the "64" direction.

Once the data have been accumulated on tape, one can use the computer to scan the tape and present the
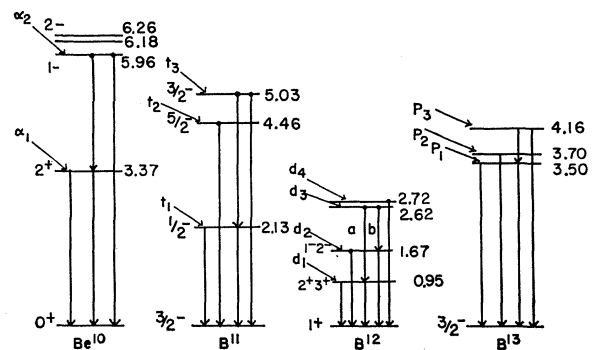

FIG. 4. Energy-level diagram of the residual nuclei capable of being formed and observed. Energies, spins, and parities are taken from the literature (except for first two excited states of B^{13}). Transitions indicated were observed.

stored information in various ways. The first, and most obvious, is simply to prepare a listing of the number of counts obtained in each of the 65 536 channels. This was done by repeatedly scanning the data tape with the computer. The 4096-word memory was used in the same way as it was used on direct storage except that a pair of 8-bit numbers was stored on a given scan only if the upper 2 bits had a given value. This would require 16 scans except that some of the memory was taken up by program so a somewhat larger number of scans was necessary. After each scan, the computer memory was put on another tape for listing on a mechanical printer. The total scanning time for data accumulated here at a rate of several per second for 10 h was about 15 min. The printing time was about 2 min for all 65 536 channels.

A second presentation resulted from a scan of the data tape in the same manner as above, for a 31×256 section out of the full 256×256 matrix and gave a contour display of the results on the oscilloscope. The 31×256 section was condensed to 31×128 with the gamma-ray detail being suppressed somewhat by dropping one bit. The section size was determined by the computer memory size. The scan time was determined by the amount of data accumulated and in this case, it was about 30 sec. Eight sections almost covered the whole matrix. This presentation served the same purpose as that used in connection with direct storage with the advantage that more detail could be studied where such detail might occur. This detailed presentation could be obtained at any time during the experiment merely by interrupting the accumulation of data and programming the computer. Accumulation proceeded after the interruption and reprogramming.
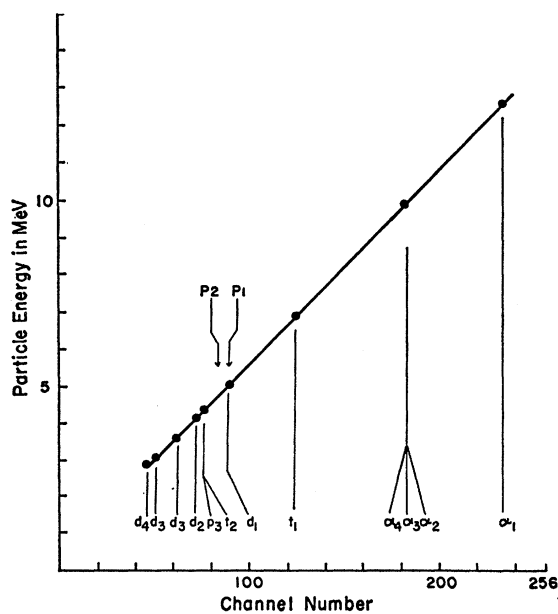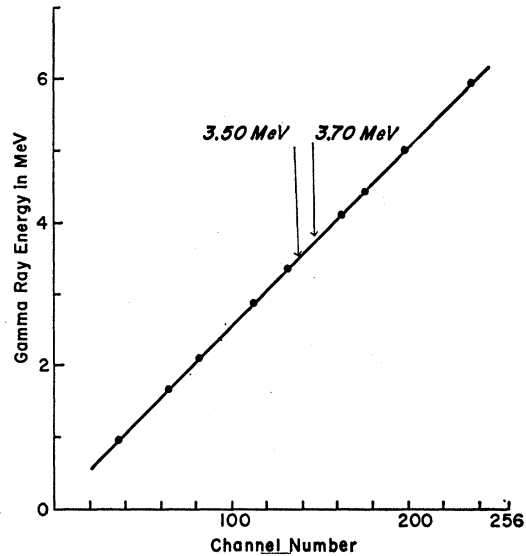

FIG. 6. Observed gamma-ray energy versus photopeak pulse height.

Another presentation of the data of considerable utility in this case was obtained by scanning the data tape in exactly the same manner as immediately above so that a 31×256 swath out of the data was condensed to 31×128 and stored in the computer memory. A selected number of rows (31) corresponding to some particle energy group was then summed over for a given column number and the result displayed as the vertical coordinate in a display where the horizontal coordinate was the column number. This was done for each of the 128 column numbers giving a 128-channel pulse-height distribution for the gamma rays in coincidence with a given energy particle group. Such pulse-height distributions show the gamma decay of a given energy level of a residual nucleus if only one particle group occurs at that energy. This is true in some cases, but in others there are two different particles of nearly the same energy. In most cases, the particle energies are sufficiently different that the gamma radiation can be easily assigned to its proper energy level especially since the kinematics of the reaction help to identify the particle identity. In a sense, this presentation gives a third dimension to the three-dimensional pulse-height analysis, two of whose dimensions appear in the contour presentation above.

RESULTS

The experimental results are given in Fig. 3 where the positions of the peaks in the 65 536-channel pulse-height analysis are shown. This is taken from the direct listing of results. Peaks are identified according to the residual nucleus giving off the gamma ray observed and the associated particle which is detected in coincidence. Peaks not so identified are one-escape peaks. A typical number of counts in a boron peak is 50 per channel and

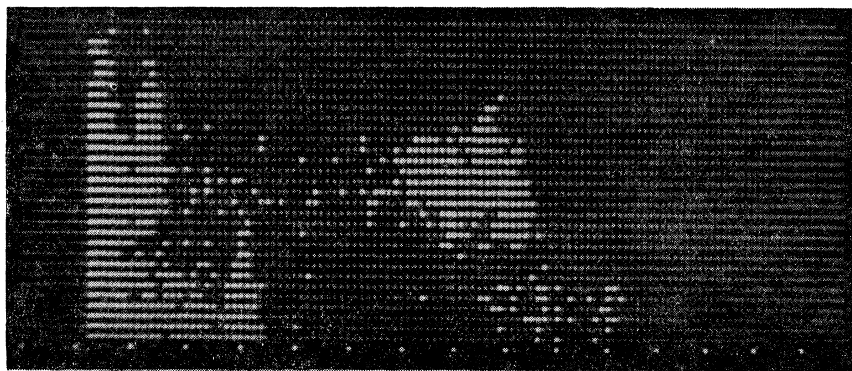FIG. 5. Observed particle energy versus pulse height.

FIG. 7. Polaroid camera picture of data represented in Fig. 3. Picture shows rows 72–102 inclusive. This includes particle energies from 4.0 to 5.6 MeV. The 256 columns in Fig. 3 are compressed to 128 (bright spots at bottom mark every eight). The bright blobs in the middle of the picture are the photopeaks and one-escape peak of the 3.50- and 3.70-MeV gamma rays from B^{13}. The four blobs run together at this contour level (12 counts). The scanty counts in the region just below these blobs are from the 4.16-MeV gamma ray from B^{13} and the 4.46-MeV gamma ray from B^{11}. The complete absence of counts for all columns below the tenth is instrumental.

a typical number of counts between peaks is 0 to 1 per channel. A typical number of channels in the region where the number of counts per channel is above half-maximum is about 30, so a peak is well defined by over 1000 coincidences.

The identification was made on the basis of the known energy levels of the residual nuclei which could contribute to the experimental results. These are shown in Fig. 4. All of the information shown, except for that about the first two excited states of B^{13}, is taken from the published literature.[1] All peaks observed are accounted for by the groups shown in Fig. 4. Calculated particle energies are plotted against observed channel number with identification in Fig. 5. The calculated energies take into account the energy loss of the particles in the aluminum backing and absorbing foil. In each case, the observed coincident gamma-ray energies are those which could arise from decay of the residual nuclear state. The gamma-ray energies are similarly plotted in Fig. 6. The linearity of the plots in Figs. 5 and 6 adds confidence to the assignments.

All of the kinematic calculations and corrections for energy loss in backing and absorbing foil for the particles detected were performed by the Model 160 computer. This computer will handle problems in fortran language.

The only exception to the fact that all peaks corresponded to previously known bound levels occurred for B^{13}. In place of a previously observed level[4] at 3.70 MeV in B^{13}, particles and gamma rays were observed which could be interpreted as associated with two closely spaced levels in B^{13} at 3.50±0.05 and 3.70±0.05 MeV. The resolution of the previous work indicating a single level was such that it could very well have not resolved two particle groups such as those observed here. It is, therefore, proposed that the previously

known first excited state of B^{13} be replaced with a doublet with 200-keV spacing.

This region of the data is shown in Fig. 7 which is a photograph of the oscilloscope contour display set at the 12-count level. This scan of the data tapes was set to cover 31 rows starting at row 72. It includes the particle groups p_3, t_2, p_2, d_1, and p_1, the first two and last two of which have the same energy at the particle detector. The gamma-ray energy coordinate is compressed by a factor of 2 in this display so there are 128 channels. Bright spots at the bottom mark every 8 channels. The rather broad extension of the peaks in the particle energy direction, in spite of detectors which showed better than one-percent resolution with natural alpha particles, is primarily caused by the target thickness (about 100-keV to 3-MeV Li ions). The variation of product energy with angle, within the detector angular acceptance, did not contribute appreciably to this extension at 0°. Also, the number of counts in the deuteron peaks are considerably higher than the contour level which means that one is quite far down the side of the deuteron peaks.

The assignment of peaks was confirmed by data taken with the particle detector at a backward angle of 140° and the gamma-ray detector at 90°. Since the particle energies in these reactions change rapidly and differently with angle for different particles, a quite different pattern of data was obtained. The same levels shown in Fig. 4, including the doublet in B^{13}, accounted for all observed peaks and all peaks predicted on the basis of the levels shown in Fig. 4 appeared.

Figure 8(a) and 8(b) shows the pulse-height distributions corresponding to the decay of each of the states in the doublet. In addition to condensing the gamma-ray coordinate by a factor of two, a sum was performed over four rows. Figure 8 is the result. Each point is the number of counts in an area 4 channels wide along the

[4] G. C. Morrison and J. A. Galey, Phys. Rev. **116**, 1583 (1959).

particle energy and 2 channels wide along the gamma-ray energy in the original data. For Fig. 8(a), the bottom row was number 87; for Fig. 8(b), it was number 82. Summing from these rows gave the maximum number of counts in the peaks of the two higher energy gamma rays. It happens that the two gamma rays in Fig. 8(a) accidentally occur at the same particle energy.

It should be added for emphasis that no new excited states were found, except in B^{13}. The known bound excited states, with this exception, sufficed to explain all peaks.

BRANCHING RATIOS

Proton Groups

Figure 8(a) shows the pulse-height distribution corresponding to the decay of the first excited state of B^{13}. Only ground-state radiation, of course, appears. Figure 8(b) shows no evidence of the presence of 3.50-MeV gamma radiation so one concludes that the 3.70-MeV state decays primarily to the ground state and less than 20% occurs by cascade.

The gamma decay of the third excited state of B^{13} is obscured in the data presented in Fig. 8(c) by the accidental equality of energy of p_3 and t_2. The ground-state-decay gamma ray can be seen in the pulse-height distribution but accurate estimates as to cascade decay are not possible because of the presence of 4.46-MeV radiation. The third excited state is apparently populated somewhat less than the first two states or the p_3 particle intensity in the forward direction is relatively

FIG. 9. Same as Fig. 8 for deuteron groups. (a) d_2, (b) d_3, (c) d_4.

weak. For the angles of observation used, there is about a factor of two less gamma decay of the 4.16-MeV state than of either the first two excited states.

The existence of cascade decay, however, is clearly shown by the presence of 0.65-MeV radiation in Fig. 8(c). This is interpreted as arising from decay to the 3.50-MeV level and estimated to occur in $(25\pm10)\%$ of the cases.

Deuteron Groups

Figure 8(a) includes the pulse-height distribution from the gamma radiation from the first excited state of B^{12} which, of course, decays 100% to the ground state. Figure 9 shows the pulse-height distribution for the second, third, and fourth excited states of B^{12}. Four-channel sums over the orginal data along the particle coordinate were performed as above. Figure 9(a) shows that the second excited state at 1.67 MeV decays 100% to the ground state. The high-energy radiation at about 4–4.5 MeV comes from the tails of peaks in coincidence with the t_2 and p_3 groups. No observable amount of 0.95-MeV radiation is present in Fig. 9(a) so less than 5% of the decay could occur by cascade. The 0.65-MeV radiation can again be accounted for by cascade decay of the 4.16 MeV state in B^{13}.

Figure 9(b) shows gamma-ray peaks at 0.95 and 1.67 MeV and a "peak" at 2.72 MeV. The latter is not maximized for particle energy, however, as the two lower peaks are. The complementary situation occurs in Fig. 9(c) where the 2.72-MeV peak is maximized but the other two are not. This is interpreted as indicating that the 2.72-MeV level in B^{12} decays directly to the ground
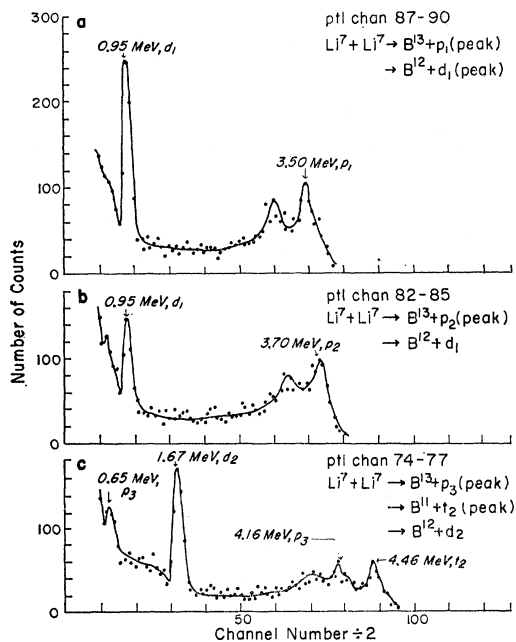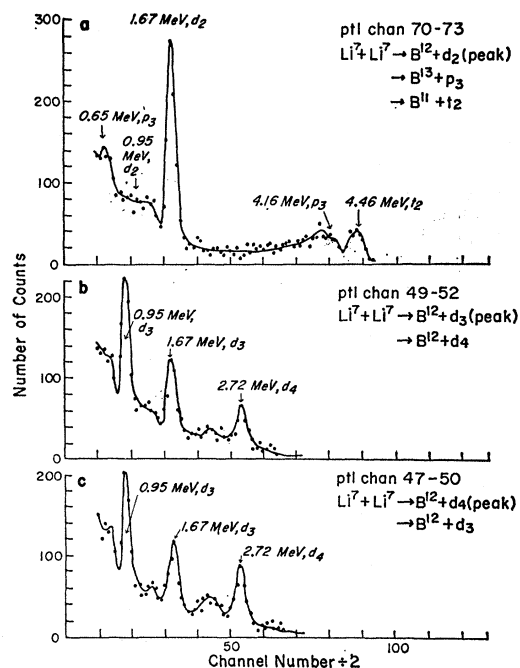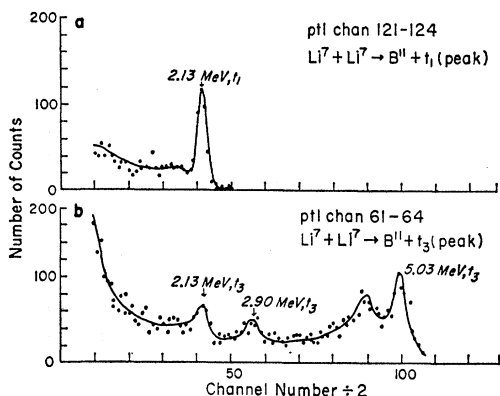
FIG. 8. Pulse-height distribution for gamma rays in coincidence with particle pulses at the peak of the various proton groups observed. Because of accidental equality of energy, a deuteron group in one case and a triton group in another have the same energy as proton groups. (a) p_1 and d_1, (b) p_2, (c) p_3 and t_2.

FIG. 10. Same as Fig. 8 for triton groups. (a) t_1, (b) t_3.

state, cascading less than 20% of the time, whereas the 2.62-MeV level decays by cascade.

The detailed nature of the cascade decay of the 2.62-MeV level in B^{12} remains in doubt, however, because of the accidental similarity of the gamma-ray energies which result from decay through the two levels of B^{12} lying below the 2.62-MeV level. This is indicated in Fig. 4 by the two alternatives (a) and (b), both of which give two gamma rays of energy about 1.67 and 0.95 MeV. The present results do not resolve this uncertainty.

Triton Groups

Figure 10 shows the pulse-height distributions in coincidence with triton groups corresponding to the first and third excited states of B^{11}. In this case, there are higher bound levels which were not observed because of insufficient energy. The results for the second excited state of B^{11} accidentally fall at the same particle energy as that for the third excited state of B^{13} with the bombarding energy, angles and foils used here. These results are shown in Fig. 8(c). There is no evidence for any cascade decay of the 4.46 MeV state of B^{11}. An upper limit of 5% on such cascade decay is indicated.

Figure 10(a) shows the ground-state transition of the first excited state of B^{11} giving the shape of the 2.13-MeV gamma-ray pulse-height distribution. Figure 10(b) shows the transition to the ground state and to the first excited state from the third excited state. No sign of a transition to the second excited state appears. The branching ratio is given in Table I.
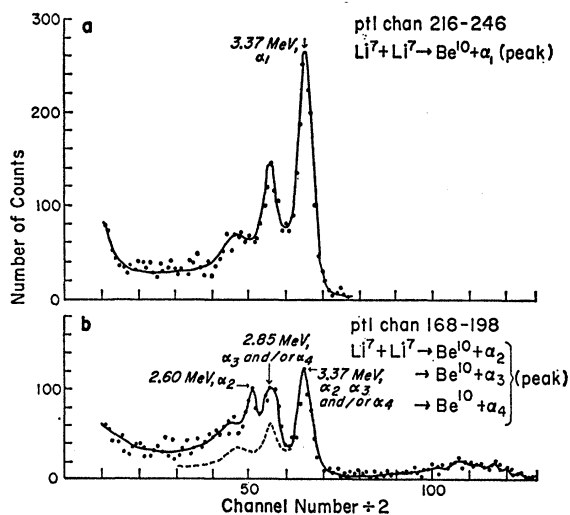
Alpha Groups

Figure 11 shows the pulse-height distributions in coincidence with alpha-particle groups. Figure 11(a) shows that corresponding to the first excited state of Be^{10} at 3.36 MeV. This pulse-height distribution is to be compared with that given in Fig. 11(b) for the groups corresponding to the three excited states at 6.0 MeV. It is obvious that at least one of these states decays by cascade through the first excited state.

TABLE I. Branching ratios for bound excited states of Be^{10}, B^{11}, B^{12}, and B^{13} (in %). Energies in MeV.

B^{13}	3.70	3.50	0		
4.16	<10	25±10	75±10		
3.70	...	<10	100		
3.50	...	...	100		
B^{12}	2.62	1.67	0.95	0	
2.72	<20	<20	<20	100	
2.62	...	b	a	<20	a+b=100
1.67	...	...	<2	100	
0.95	...	...	...	100	
B^{11}	4.46	2.13	0		
5.03	<5	15±5	85±5		
4.46	...	<5	100		
2.13	...	...	100		
Be^{10}	3.37	0			
5.96	75±10	25±10			
3.37	...	100			

The poor resolution resulting from target thickness made it impossible to separate the pulse-height distributions resulting from decay from each of the these excited states of Be^{10} or to determine whether all three states were formed. The pulse-height distribution shown in Fig. 11(b) is the result of summing over all of the $\alpha_{2,3,4}$ particle groups. As Fig. 12 shows, there is no structure obvious in this particle group, although it is wider than one would expect for a single alpha-particle group on the basis of the width of the first excited state alpha group shown in Fig. 12. Figure 11(b) shows evidence of the cascade decay of the 5.96-MeV excited state in Be^{10} in the presence of the 2.60-MeV gamma ray. The ground-state decay of this state also appears to be present. An estimate of the branching ratio is given in Table I.

One or both of the two states of Be^{10} at 6.18 and 6.26 MeV are populated as well as the state at 5.96 MeV.

FIG. 11. Same as Fig. 8 for alpha groups. (a) α_1, (b) $\alpha_2\alpha_3\alpha_4$.
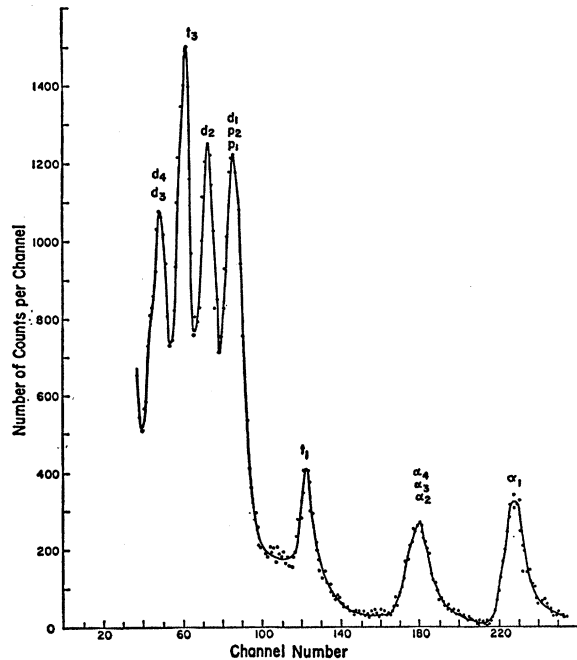
FIG. 12. Particle-detector pulse-height distribution for pulses in coincidence with gamma radiation. Each point is the result of summing all counts in a row in Fig. 3.

The peak at the position of the one-escape peak of the 3.37-MeV gamma ray is too large to be solely of this origin. There is a perfect example for comparison in Fig. 11a. Gamma radiation resulting from cascade decay of the 6.18- and 6.26-MeV states give gamma rays of 2.81 and 2.89 MeV, respectively. Their photopeaks add to the one-escape peak of the 3.37-MeV gamma ray. Since the two states are not resolved, no branching ratio is given.

CONCLUSION

The branching ratios in Table I can be compared with previous measurements in the cases of Be¹⁰ and B¹¹. These are summarized in Ajzenberg and Lauritsen's review article.[1] For the B¹¹ case, a more recent work was done to redetermine these branching ratios and those for the corresponding levels in C¹¹.[5] The present results, for both Be¹⁰ and B¹¹ are in good agreement with these previous determinations.

The nature of the gamma emission from the bound levels of B¹² and B¹³ is new information. In the case of B¹², stripping reaction studies[6] have placed limitations on the spin and parity of the 0.95- and the 1.67-MeV state. The former is $\leq 3+$ and the latter is 2^- or 1^-. Further limitation of choices for the 0.95-MeV state result from studies[7] of the angular distribution of the gamma radiation following the (d,p) reaction. This

limits the choices for the 0.95-MeV level to $2+$ and $3+$. Since the ground state is $1+$, a choice of $3+$ and $1-$ for the 0.95- and 1.67-MeV states would result in a greatly favored ground-state decay as opposed to cascade decay. The other three sets of spin and parity choices give $E1$ transitions from the 1.67-MeV state to both the 0.95-MeV state and the ground state. The ground-state decay would only be favored by the extra energy available. One would expect about 8% cascade decay. The 2% upper limit on this cascade decay is not enough to rule out these possibilities, if one takes into account the possible range of $E1$ matrix elements.[8] Actually, a choice of $2+$ and $2-$ would fit nicely with corresponding levels in C¹².[9] The results for the first two excited states of B¹² are, therefore, consistent with what is known but await more complete knowledge of spins to be useful.

This is even truer of the closely spaced doublet of levels in B¹² at 2.62 and 2.72 MeV for which there is no information on spin and parity. They decay in strikingly different ways. The level at 2.62-MeV decays by cascade decay through the lower levels while the level at 2.72-MeV decays by a ground-state transition. The cascade decay of the 2.62-MeV level shows up an interesting "accident" in the energy-level structure of B¹² in that, within the uncertainties in energy, cascade decay from this level through either of the two lower excited states produces two gamma rays of the same energy. It is for this reason that it was only possible to say that this state undergoes cascade decay but not how it does so.

The excited states of B¹³ are entirely undetermined as to spin and parity. The present experiment shows two states in place of one previously observed—3.50 and 3.70 MeV. The pattern of branching ratios for all the bound states of B¹³ bears a certain resemblance to that observed for B¹¹. This leads to the tempting conjecture that the spins and parities of the first three excited states of B¹³ are the same as those of the first three levels of B¹¹. The ground states have the same spin and parity. On a simple independent particle model, one would expect the low-lying states in both cases to arise from the configuration of three protons in the $1p$ shell. This configuration gives five states—one with spin $\frac{1}{2}^-$, three with $\frac{3}{2}^-$, and one with $\frac{5}{2}^-$—which cover the known cases in B¹¹. Whether they also cover the case in B¹³ is uncertain, especially since rough estimates[10] show that only two of these five states lie below 7 MeV in B¹³.

In summary, the two-parameter-analysis technique makes possible the simultaneous study of a number of nuclear energy levels, and the branching ratios for gamma-ray decay of bound levels of Be¹⁰, B¹¹, B¹², and B¹³ have been investigated using this technique.

[5] P. F. Donovan, N. Kane, R. E. Pixley, and D. H. Wilkinson, Phys. Rev. 123, 589 (1961).

[6] J. R. Holt and T. N. Marsham, Proc. Phys. Soc. (London) A66, 1032 (1953).

[7] E. Kondaiah and C. Badrinathan, Nucl. Phys. 15, 254 (1960).

[8] D. H. Wilkinson, in Proceedings of the Rehovoth Conference on Nuclear Structure, edited by H. J. Lipkin (North-Holland Publishing Company, Amsterdam, 1957).

[9] F. Ajzenberg and T. Lauritsen, Ann. Rev. Nucl. Sci. 10, 409 (1960).

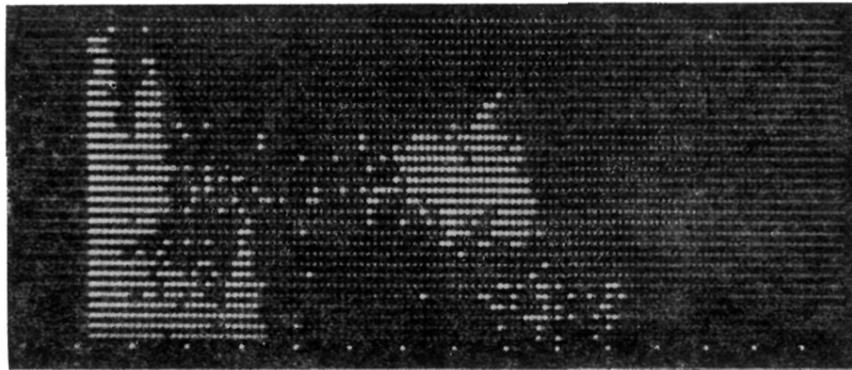[10] I. Talmi and I. Unna, Ann. Rev. Nucl. Sci. 10, 353 (1960).

FIG. 7. Polaroid camera picture of data represented in Fig. 3. Picture shows rows 72–102 inclusive. This includes particle energies from 4.0 to 5.6 MeV. The 256 columns in Fig. 3 are compressed to 128 (bright spots at bottom mark every eight). The bright blobs in the middle of the picture are the photopeaks and one-escape peak of the 3.50- and 3.70-MeV gamma rays from B^{13}. The four blobs run together at this contour level (12 counts). The scanty counts in the region just below these blobs are from the 4.16-MeV gamma ray from B^{13} and the 4.46-MeV gamma ray from B^{11}. The complete absence of counts for all columns below the tenth is instrumental.